Journal of the European Ceramic Society **18** (1998) 1153–1160

PII: S0955-2219(98)00037-5
0955-2219/98/$—see front matter

Properties of Nanocrystalline Ceramic Powders Prepared by Laser Evaporation and Recondensation

U. Popp,[a]* R. Herbig,[a] G. Michel,[ab] E. Müller[a] and Ch. Oestreich[a]

[a]Institute of Ceramic Materials, Freiberg University of Mining and Technology, D-09596 Freiberg/Sa., Germany
[b]Institute of Technology, Friedrich-Schiller University Jena, D-07743 Jena, Germany

Abstract

Nanocrystalline ceramic powders (ZrO_2, Al_2O_3, Si_3N_4, AlN) are prepared by evaporation of solid materials (sintered rods or coarse powder) in thefoeus of a CO_2 laser and the following recondensation in a carrier gas stream. The production rates are in the range of 40–100 g h^{-1} (cw mode, oxides) or more than 200 g h^{-1} (cw mode, nitrides), respectively. The particle size distribution can be influenced by different parameters of the formation process like laser power, area of the laserfocus, pulse length in case of pw mode, streaming velocity and type of the carrier gas. The powders consist of nearly spherical particles with diameters in the range of 10–100 nanometers. Features of the produced alumina and zirconia powders are reported concerning phase transformation, behaviour in suspensions and processing properties. © *1998 Elsevier Science Limited. All rights reserved*

1 Introduction

It is known, that the sinter behaviour and the properties of sintered ceramics decisively depend on particle size, size distribution and particle shape of the used powders. Therefore, today many research groups are engaged in producing nanopowders with narrow particle size distributions and slight agglomeration behaviour.

By using optimised granulation and sintering parameters such powders can be densified in order to achieve dense ceramics with submicrograin structure and small grain size distributions, which show excellent and partially unusual mechanical behaviour like superplasticity or machinability.

However, the milling and grinding methods for producing such nanopowders are limited with regard to the attainable fineness of the powders, but also by pollution. Powders produced by chemical procedures often show agglomeration behaviour unfavourable for the sintering process: for instance, powders produced by laser assisted chemical vapour precipitation technique are often inhomogeneous in their atomic structure and composition. Another example is the pyrolysis of metal halides, whereby the produced powders show a strong tendency to agglomerate because of their surfaces with a high content of hydroxyl groups.

Finally, many nonmechanical methods for producing nanopowders are strongly limited with regard to their yield rates.

Hence, efficient methods for producing sinterable nanopowders are required, but there is also an urgent need of investigations with regard to handling and processing of such powders.

In this paper, we want to give some information about production process and properties of nanopowders produced by evaporation in the focus of a laser beam and the recondensation in the stream of an inert (Ar, He) or reactive (O_2, N_2) carrier gas. This method was already described by Kato[1] and used by Mordike *et al.*[2,3] In our case, in this way nanopowders with interesting technological properties are produced under reaching relatively high evaporation rates in comparison with similar methods.

2 Experimental

As reported already in the past[4,5] we used a transverse flow CO_2 laser GTL 480,[6] because its

*To whom correspondence should be addressed.

wavelength of the emitted laser beam $\lambda = 10{\cdot}6\,\mu m$ is strongly absorbed by our ceramic materials. The laser is characterized in the cw operation mode by the following parameters:

- laser output power: 1–4 kW
- diameter of the laser beam: 40 mm
- electro-optical efficiency: 11%
- total electrical supply: 70 kW (for resistance stabilized discharge).

Figure 1 shows the principles of the two available chambers for the evaporation of (a) bulk material or (b) coarse powders, respectively. It could be shown, that the highest evaporation rate (mass m per time t) was reached, if the focal plane coincides with the surface of the target. The focussion of the radiation was realized by a spherical mirror (focal length $f = 150$ cm).

In case of pw mode by two different Q-switching techniques it is possible to generate the length of the pulses between 1 and 500 μs:

- By using a rotating chopper disk placed in the focal plane of an intracavity telescope pulses with a distinct peak nearly 150 ns duration and 50 kW peak power can be generated at repetition rates of a few kHz.
- A modified resonator allows to modulate the high output power of the laser. The pulse shape is characterised by a peak of about 1 μs and a following 'tail' whose time duration can be varied over a wide range.

Figure 2 shows the dependence of zirconia evaporation rates on the pulse length and the average power P of the two types of Q-switched pulses in comparison with the results by using the cw mode.

Oxides have been produced in air, oxygen or argon atmosphere, the nitrides in a carrier gas stream of nitrogen.

The nanopowders have been characterized concerning their granulometric parameters, their phase transformation behaviour and their processing parameters. Some of these results are reported.

3 Results

3.1 Characterization of the produced nanoparticles (cw mode)

3.1.1 Zirconia (ZrO_2)

Figure 3 was taken by a transmission electron microscope Philips CM 30 and gives an impression of the nearly ideally spherical shape of the isolated free zirconia particles. At evaporation rates of 95 g h^{-1} the d_{50} values (calculated from TEM images) are in the range of 10–50 nm , and the specific surface area S_{BET} amounts to 15–35 m^2 g^{-1}. It can be observed (Fig. 3), that the recondensed zirconia particles are crystalline, significant amorphous contents could not be detected neither by XRD nor by microdiffraction of singular particles and tilt experiments (TEM). Our measurements by X-ray diffraction (CuK_α) showed a surprisingly high tetragonal volume content of 45–90% depending on the laser parameters, which already has been reported elsewhere.[7] That means, that caused by the rapid cooling of these particles after the laser evaporation process in case of nonstabilised zirconia the transformation tetragonal→monoclinic mostly not happened.

3.1.2 Alumina (Al_2O_3)

As shown in Fig. 4, also the produced Al_2O_3 nanoparticles (evaporation rate 75 g h^{-1}) are spherical shaped with a specific surface area $S_{BET} = 53$ m^2 g^{-1} and d_{50} values of 18–20 nm. They are characterized by a narrow particle size distribution with $d_{10} = 9$ nm, $d_{50} = 18$ nm and

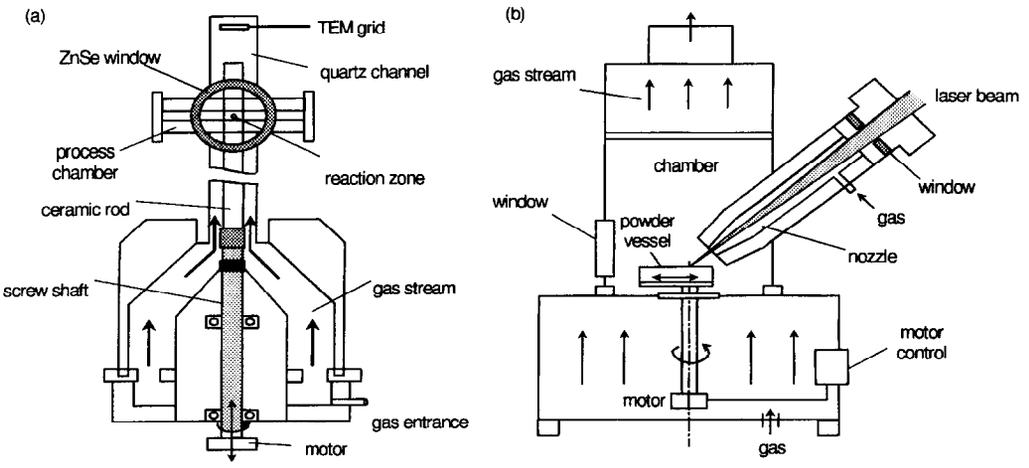

Fig. 1. Schemes of the evaporation chambers for (a) rods and (b) coarse powders.

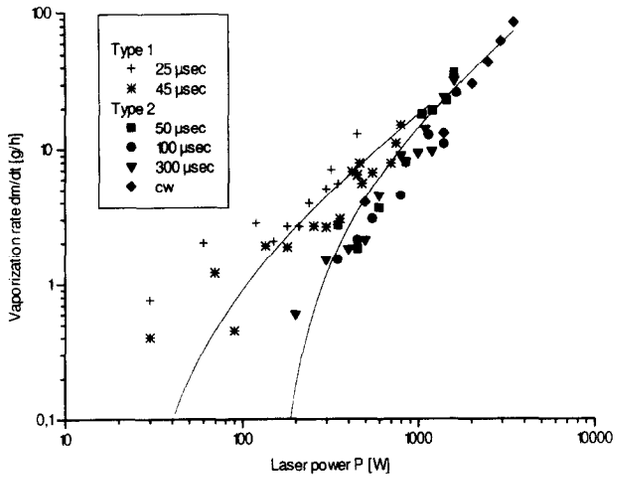

Fig. 2. Evaporation rate dm/dt of zirconia as a function of the laser power P.

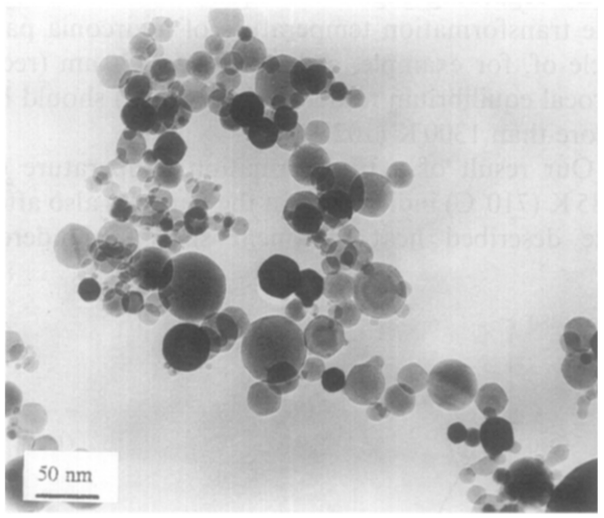

Fig. 3. TEM image of laser evaporated zirconia.

$d_{90} = 32$ nm (Fig. 5). Also in this case we find crystalline particles (γ- and δ-alumina) by XRD investigations. The ratio of both modifications is about 1:2.

3.1.3 Silicon nitride (Si_3N_4)

Caused by the decomposition of the silicon nitride without melting during the evaporation process and by an only uncomplete renitridation in the nitrogen gas stream the produced powders exhibit a high content of free silicon, which depends on the process parameters. XRD investigations show sharp peaks for silicon, α- and β-Si_3N_4, but also a significant underground, what indicates amorphous parts. By analysis using ^{29}Si MAS NMR Si_3N_4, silicon and SiO_2 are detectable, but no indication to $Si_xN_yO_z$ can be found. The specific surface area is $23\,m^2g^{-1}$ at a relatively high evaporation rate of $200\,g\,h^{-1}$. Since the powders consist of a mixture of SiO_2, silicon and Si_3N_4 there are some problems to measure the size distribution of the silicon nitride particles by TEM. An impression of shape and agglomeration behaviour of the powders is given in Fig. 6. These first experiments show that it is possible to produce silicon nitride nanoparticles in that way.

3.1.4 Aluminium nitride (AlN)

In distinction from silicon nitride in case of AlN a melt exists under a nitrogen atmosphere. Therefore, at the first stage of the recondensation process liquid droplets of the final composition AlN may be formed and the produced nanopowders do not show any content of free aluminium, but a content of more than 11 wt% oxygen caused by oxygen pollutions of the nitrogen atmosphere. Using XPS analysis it can be assumed, that there are different bonding states of the aluminium at the surface of the particles ($Al(OH)_3$, AlO(OH), etc.). The evaporation rate amounts to $230\,g\,h^{-1}$, the specific surface area is in the range of 35 m^2/g^{-1} (Fig. 7). Typical particles are nearly spherical with a diameter lower than 100 nm. The finest particles are partially agglomerated and show different morphologies. A significant amorphous part could not be detected by XRD.

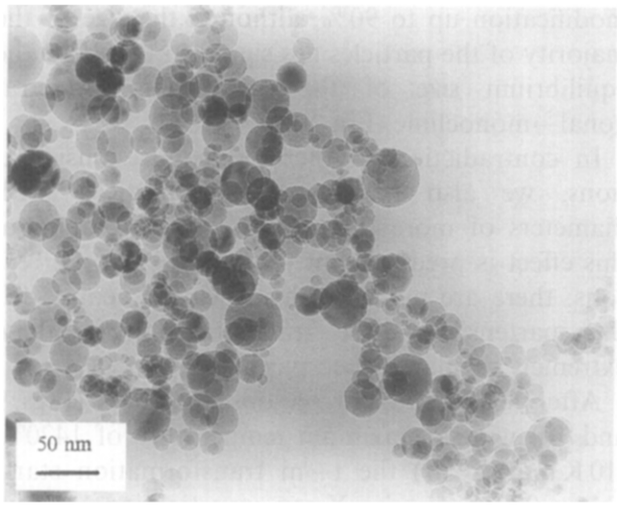

Fig. 4. TEM image of laser evaporated alumina.

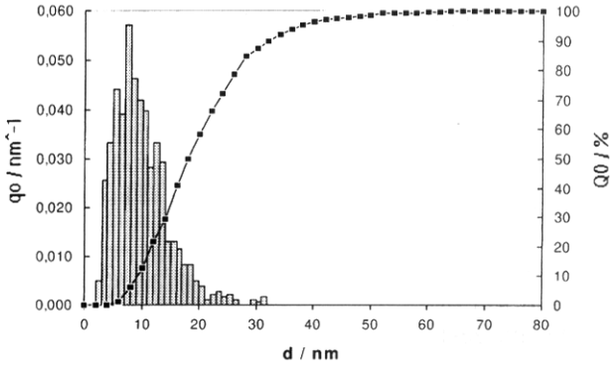

Fig. 5. Particle size distribution (by number) of laser evaporated alumina.

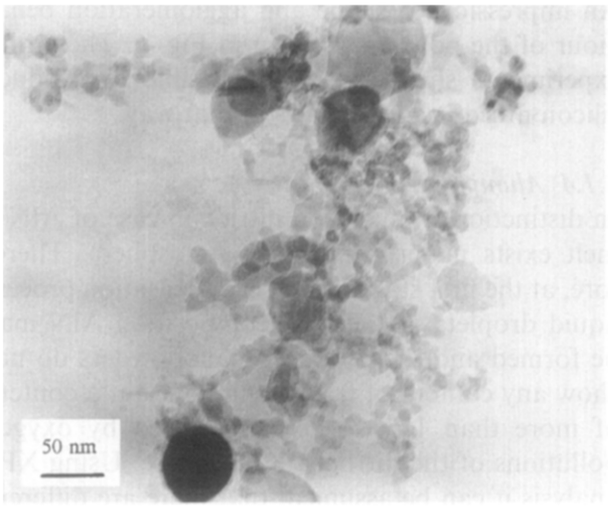

Fig. 6. TEM image of laser evaporated silicon nitride.

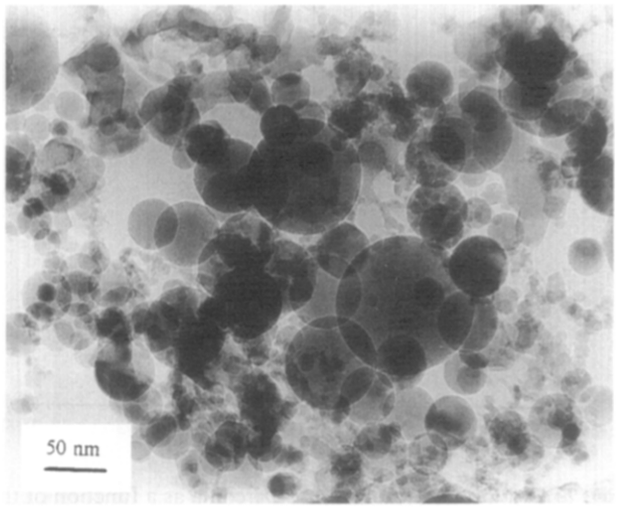

Fig. 7. TEM image of laser evaporated aluminium nitride.

3.2 Special properties of alumina and zirconia nanopowders

3.2.1 Phase transformation behaviour and granulometric properties of zirconia in dependence on a following heat treatment

As we published elsewhere[7] the laser evaporated and recondensed pure, nonstabilized zirconia powders show a high volume part of the tetragonal modification up to 90%, although the size of the majority of the particles lies significantly above the equilibrium size of the transformation tetragonal→monoclinic (Fig. 8).

In contradiction to thermodynamic considerations, we also find tetragonal particles with diameters of more than 100 nm. In our opinion, this effect is predominantly caused by kinetic reasons: there are not enough nucleation centres for the martensitic phase transformation in these extremely regular shaped particles.

After heat treatment of loose powders (Figs 9 and 10) with a maximum temperature of 1420°C (10 K min^{-1}, air) the t→m transformation starts below 920°C (*in-situ* X-ray investigations). Lowering the maximum temperature, we could notice, that the transformation temperature decreases as follows:

Annealing until a maximum temperature of	**1010°C**	**1070°C**
t→m transformation temperature	610°C	710°C
Average chord length of the particles (evaluation of TEM images)	69 mm	116 mm

Figure 11 illustrates the chord length distributions of the investigated powders after heat treatment.

By regarding Fig. 8 for equilibrium conditions the transformation temperature of a zirconia particle of, for example, a diameter $d = 120$ nm (reciprocal equilibrium radius $= 16 \times 10^6$ m^{-1}) should be more than 1300 K (1025°C).

Our result of a transformation temperature of 985 K (710°C) indicates, that the particles also after the described heat treatment show a hindered

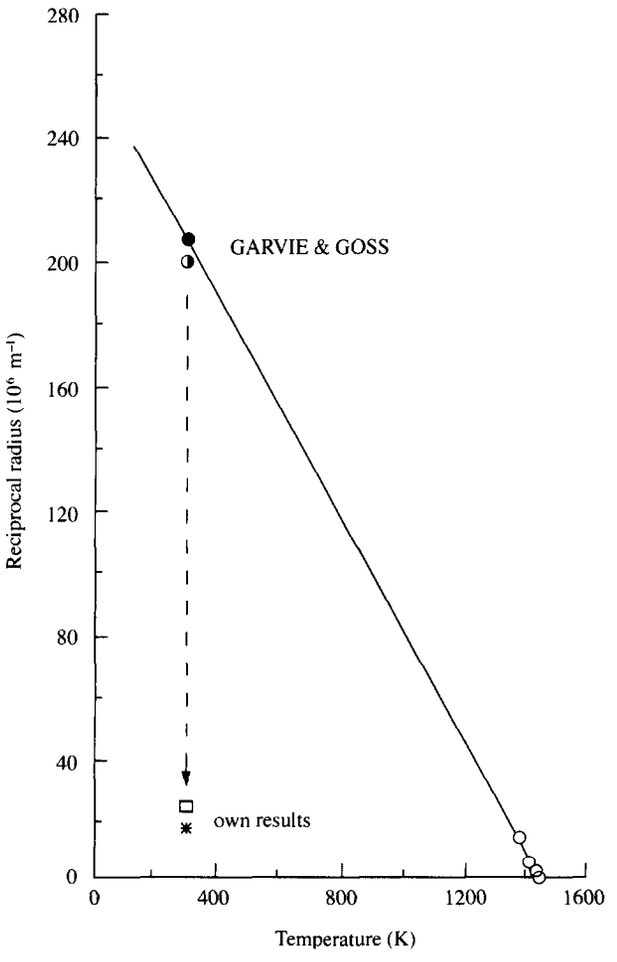

Fig. 8. The reciprocal equilibrium radius of the t -> m transformation of zirconia in dependence on the temperature (○, ●, inclined line: from[11], □, *, Δ: own results).

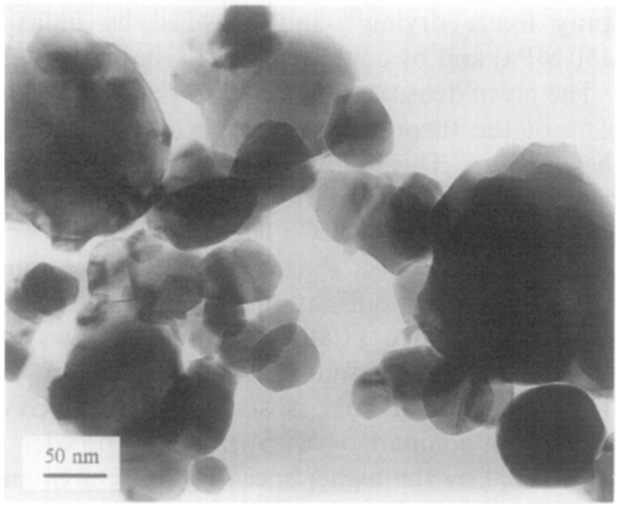

Fig. 9. TEM image of zirconia particles after a heat treatment of 1010°C.

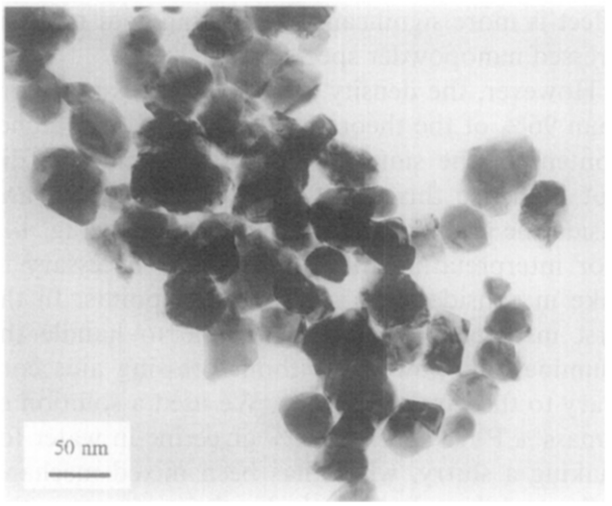

Fig. 10. TEM image of zirconia particles after a heat treatment of 1070°C.

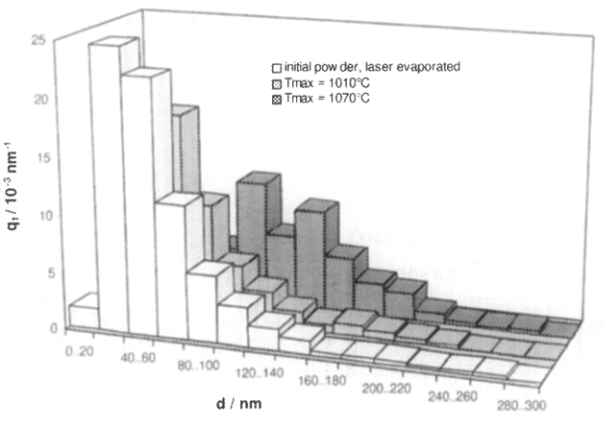

Fig. 11. Chord length distribution of the particle size after a heat treatment in comparison with the starting powder.

transformation behaviour caused by their relatively regular shapes, i.e. by a lack of nucleation centres. It can be assumed, that there is no significant obstacle of transformation by changed stoechiometry of the powders, because a possible oxygen addition occurs only in the temperature range of 200–300°C during heating in air, which is typical for a small oxygen deficit only in the surface region.

Compacted powders do not show the effect of hindered transformation because of the beginning sintering, what means that unregulary shaped grains with a greater dimension are transformed rather than in case of loose powders.

At room temperature the transformation is finished; the powder modification now is monoclinic.

3.2.2 Acustophoretic investigations of laser evaporated and initial zirconia and alumina powders

The kind of the atmosphere during the laser evaporation and recondensation process can significantly influence the properties of the nanopowders. Measurements of the ζ-potential by the ESA method (Matec ESA 8000) show that the behaviour of e.g. zirconia nanopowders in suspensions are changed, if the atmosphere during the laser process is altered from O_2 to Ar:O_2 = 1:1 to Ar.[8]

Another interesting point of view is the comparison of the behaviour of the initial zirconia and alumina powders with them of the produced nanopowders in deionised water in dependence on pH.

We found, that the change of the dynamic mobility of the initial powders is characterised by a relatively constant rising trend versus pH (Fig. 12).

In comparison with that, the nanopowders show a steep rising, what means, that the sign of the charge of these particles changes during a small pH range. Caused by a great difference between the isoelectric points of the laser evaporated alumina and zirconia, for the nanopowders there is a wider pH range (II) with contrary charge of the alumina respectively zirconia particles and so for producing of stable Al_2O_3–ZrO_2 suspensions (using the effect of heteroflocculation) than in the case of the initial powders (I).

What could be the reasons of these results?

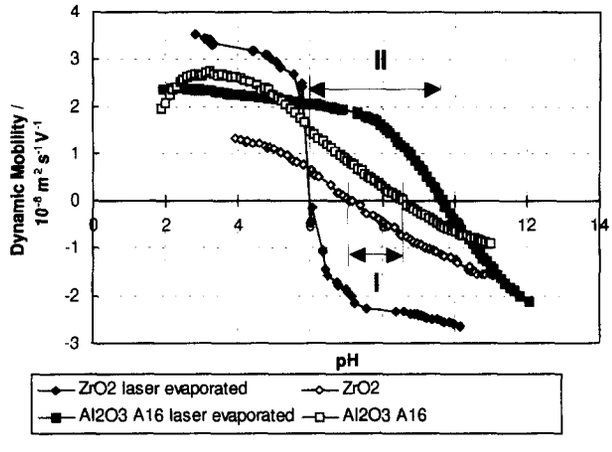

Fig. 12. Dynamic mobility versus pH for initial and laser evaporated ZrO_2 and Al_2O_3 powders.

In YTZ nanopowders produced in the same way, we found in the surface a sodium content of about 2 at% by XPS, whereby by ICP-OES an Na content lower than 0·020 at% is found.[8] For interpreting this difference we assume that the sodium impurities originally homogeneously distributed in the bulk after the laser process are concentrated at the surface of the nanopowders for lowering the surface energy. That is why we find a higher content of Na by XPS than by ICP-OES, which will influence the pH dependence of the ESA signal in a specific way.

We suppose that the same effect occurs also in pure zirconia and is responsible for the different ESA results for initial and nanopowders.

In our investigations it can be observed that in the case of comparable powders the dynamic mobility increases, if the grain size decreases.[9] For Al_2O_3 a higher content of fine grains shifts the isoelectric point towards a higher pH.

Besides, the sharp decreasing of the dynamic mobility of the nanopowders shows that the OH^- groups at the surface of the fine powders have more uniform bonding properties than in the case of the initial powders, which is responsible for the nearly simultaneous changing of the behaviour of the nanoparticles surface.

3.3 Processing properties of zirconia and alumina

3.3.1 Zirconia (ZrO_2)

A nanoscaled yttria stabilized zirconia powder (2·4 mol% Y_2O_3, $S_{BET}=22\,m^2\,g^{-1}$) was densified by uniaxial pressure (20 MPa and 150 MPa, respectively) or by cold isostatic pressing (1 GPa).

For avoiding impurities we did not apply at pressing and sintering aids. The powders have been pressed and mortared before the final press procedure, and we got green densities in the range of 50 to 60% of the theoretical density in dependence on the pressure.

The pressureless sintering process in air has been characterised by a heating rate of $10\,K\,min^{-1}$, a heating stop at 1250°C (2 h) and a maximum temperature of 1400°C. In this way, we reached maximum sinter densities of 5·87–5·94 $g\,cm^{-3}$ (maximum 98% of the theoretical density). The nanopowder showed a high sinteractivity. The densification started already at 1000°C (uniaxial pressed samples) or 900°C (cold isostatic pressed samples) and was finished at 1250°C. Superplastic behaviour of the sintered specimens could be established.[8]

3.3.2 Alumina (Al_2O_3)

Laser evaporated alumina powder (mixed with 0·5 mass% MgO) has been granulated by using spray freeze drying[10] and densified by uniaxial (150 MPa) and by cold isostatic (1 GPa) pressing.

The green densities amounted to between 51 and 62% of the theoretical density in dependence on the pressure. The following sinter procedure was realised in air with a heating rate of $10\,K\,min^{-1}$ up to 1500°C (3 h) or 1700°C (3 h).

The sintering effect started only after the transformation of the modification ($\gamma, \delta \rightarrow \alpha$, that means in this case above 1100°C. Figure 13 shows the densification behaviour of uniaxial pressed (150 MPa) and of cold isostatic pressed (1 GPa) powders in comparison with the initial powder A 16. Caused by the higher specific surface area and the resulting higher sinteractivity of the regular shaped nanoparticles, in this case the densification starts at a lower temperature (1100°C) than in case of the initial powder (higher than 1200°C). This effect is more significant when using cold isostatic pressed nanopowder specimens.

However, the density after sintering is not more than 96% of the theoretical density. Also a higher content of the sintering aid MgO (1 mass%) did not influence this result. The pores between and inside the grains could not be eliminated (Fig. 14). For interpretating these results it is necessary to take in consideration the following points: In the first instance, it was not possible to handle the alumina nanopowders without pressing aids contrary to the case of zirconia. We used a solution of 1 mass% PVA and 1 mass% glycerine in water for making a slurry, which has been mixed mechanically and by ultrasound. In the next step, this slurry has been shock frozen by spraying in liquid nitrogen and freeze dried. The resulting spherical, good rippling granulates are weak and can be destroyed by pressing. However, it is possible, that

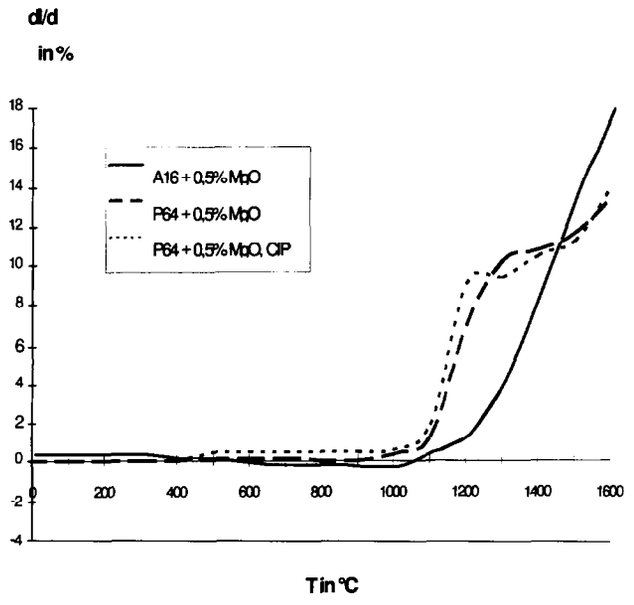

Fig. 13. Densification behaviour of alumina nanopowders in comparison with the initial powder versus temperature.

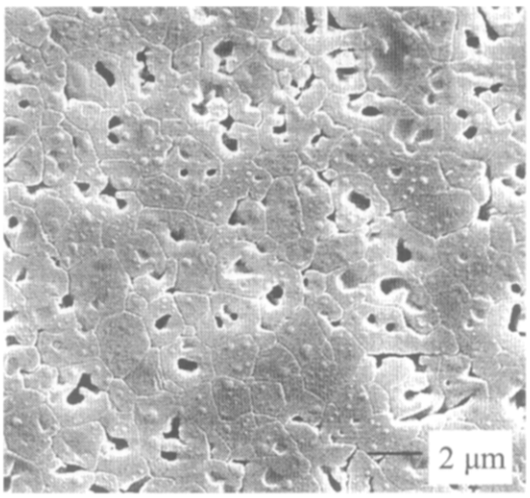

Fig. 14. Scanning electron micrograph of alumina (CIP 1 GPa, sintering temperature 1500°C).

these granulates enclosed a higher content of air caused by the very fine powders and showed by a high stretching back during pressing. After that, the organic components must be removed at 800°C (1 h) leaving pores.

On the other hand, the dilatometric investigations (Fig. 13) show, that in the case of the nanopowders (P 64) the first densification occurs between 1050 and 1200°C, caused by the transformation $\gamma, \delta \rightarrow \alpha$. In this step, small σ- and γ -particles are changed in greater α-particles, whose existence is necessary for the following sinter process, whereby pores are enclosed.

By experiments with α-alumina particles as vaccinal nuclei the phase transformation temperature could be decreased. In this case the density of the specimens at 1300°C already reached 94% of the theoretical density. However, even at a sinter temperature of 1700°C it also accounted only 96% of the theoretical density.

So it can be observed that the densification of the nanopowder specimens (especially in the case of cold isostatic pressed bulks) begins earlier than in the case of initial powder specimens (A 16), but it is not possible to realise dense ceramic specimens in this way.

A possible application of these powders is as carriers for high temperature catalysators because of their high thermal stability and their low changement of the specific surface area up to 1000°C.

4 Conclusions

The method of evaporating solid oxide and non-oxide materials in the focus of a laser is suitable for producing nanosized ceramic powders with diameters in the range of 10 to 100 nm. Evaporation rates and particle size distribution can be controlled over a wide range by varying different process parameters.

The produced particles (ZrO_2, Al_2O_3, Si_3N_4, AlN) are crystalline, mostly spherically shaped and isolated free caused by laser evaporation and recondensation of separate particles without chemical bonding between them. In comparison with the initial powders these nanoparticles show partially unusal properties with regard to phase transformation, stability in suspensions and handling during processing.

The high acitivity of the powder surfaces causes a decreasing of the starting temperature of the sinter process, but the strong agglomerates obviously induced by powder processing often hinder the elimination of microporosity. That is why it is not possible to realise fully densified ceramic specimens of these alumina powders by conventional technology. Such powders could be applied for producing ceramic carrier materials for high temperature catalysators (AL_2O_3) or for composites by co-firing with lower melting components (ZrO_2).

Acknowledgements

The authors are grateful to the Deutsche Forschungsgemeinschaft for its financial support of this research, to Professor Thomas (Institute for Analytical Chemistry, Freiberg University of Mining and Technology) for the NMR measurements and Dr Simon (Institute of Polymer Research, Dresden) for XPS investigations.

References

1. Kato, M., Preparation of ultrafine particles of refractory oxides by gas evaporation method. *Japan J Appl. Phys.*, 1976, **15**, 757–760.
2. Lee, H.-Y., Riechemann, W. and Mordike, B. L., Sintering of nanocrystalline ZrO_2 and zirconia toughened alumina (ZTA). *Journal of the European Ceramic Society*, 1992, **10**, 245–253.
3. Lee, H.-Y., Riechemann, W. and Mordike, B. L., Charakterisierung von laserzerstäubten nanoskaligen Oxidpulvern. *Z. Metallkd.*, 1993, **84**, 79–84.
4. Müller, E., Oestreich, Ch., Popp, U., Michel, G., Staupendahl, G. and Henneberg, K. H., Characterization of nanocrystalline oxide powders prepared by laser evaporation. In *Proceedings of the 4th Conference of the European Ceramic Society, Vol. 1: Basic Science—Developments in Processing of Advanced Ceramics I*, ed. C. Galassi, Riccione, Italy. Gruppo editoriale faenza editrice, Faenza, 1995, pp. 219–224.
5. Müller, E., Oestreich, Ch., Popp, U., Michel, G., Staupendahl, G. and Henneberg, K. H., Characterization of nanocrystalline oxide powders prepared by CO_2 laser evaporation. *KONA—Powder and particle (Osaka)*, 1995, **13**, 79–90.
6. Triebel, W., Ose, E., Michel, G. and Petrich, A., Experimental and theoretical investigation of a transverse flow CO_2-laser. *Proceed. SPIE*, 1988, **1031**, 41–47.

7. Oestreich, Ch., Müller, E., Schreiber, G., Michel, G. and Henneberg, K.-H., Diffraction studies on the size dependence of the t→m transformation of zirconia. *Fresenius J. Anal. Chem.*, 1994, **349**, 155–157.
8. Müller, E., Oestreich, Ch., Popp, U., Herbig, R., Michel, G. and Rendtel, A., The influence of the preparation conditions of nanocrystalline zirconia on powder processing and ceramic properties. *Key Engineer. Mater. (Euro Ceramics V)*, 1997, **132–136**, 169–172.
9. Herbig, R., Optimization of ceramic slurries by ESA measurement. In *Proceedings of the 4th Conference of the European Ceramic Society, Vol. 2: Basic Science—Developments in Processing of Advanced Ceramics II*, ed. C. Galassi, Riccione, Italy. Gruppo editoriale faenza editrice, Faenza, 1995, pp. 39–46.
10. Moritz, T., Sprühgefriergranulierung von Siliciumnitridpulvern aus nichtwäßrigen Suspensionen. Dissertation, TU Bergakademie Freiberg, 1994.
11. Garvie, R. C. and Goss, M. F., Intrinsic size dependence of the phase transformation temperature in zirconia microcrystals. *Journal of Materials Science*, 1986, **21**, 1253–1257.